HHS Public Access

Author manuscript

Materialia (Oxf). Author manuscript; available in PMC 2020 June 01.

Published in final edited form as:

Materialia (Oxf). 2019 June ; 6: . doi:10.1016/j.mtla.2019.100348.

The effect of hyaluronic acid on the corrosion of an orthopedic CoCrMo-alloy in simulated inflammatory conditions

S. Radice[1], **J. Yao**[2], **J. Babauta**[3], **M. P. Laurent**[1], and **M. A. Wimmer**[1]

[1]Rush University Medical Center, Department of Orthopedic Surgery, 1611 W. Harrison Street, Chicago, IL 60612, USA

[2]University of Washington, Department of Orthopaedic Surgery and Sports Medicine, 401 Broadway, Seattle, WA 98122, USA

[3]Washington State University, The Gene and Linda Voiland School of Chemical Engineering and Bioengineering, Wegner Hall, PO Box 646515, Pullman, WA 99164-6515, USA

Abstract

During joint inflammation, various reactive oxygen species (ROS) are present in the surrounding tissue and joint fluid. In the laboratory, hydrogen peroxide (H_2O_2) is typically used to simulate inflammatory conditions, and media containing proteins and hyaluronic acid (HA) are employed to simulate joint synovial fluid. Electrochemical interactions between H_2O_2 and HA in the presence of a CoCrMo surface are expected, since HA molecules contain redox-active moieties. We hypothesized that any redox reactions of these moieties with ROS will mitigate the oxidizing effect of H_2O_2 on the CoCrMo surface, limiting the corrosion rate of the metal.

Non-destructive electrochemical measurements (open circuit potential, linear polarization resistance and electrochemical impedance spectroscopy) were used to investigate the corrosion response of CoCrMo in synovial model fluid containing physiologically relevant concentrations of albumin proteins and hyaluronic acid, with and without H_2O_2. Two different molarities of H_2O_2, 3 mM and 30 mM, were tested. While both molarities are within physiological limits, 3mM is well within the range HA could mitigate, whereas 30 mM is not.

Contrary to our hypothesis, HA did not alleviate corrosion in 3 mM H_2O_2 and even caused a corrosion increase in the case of 30 mM H_2O_2. The decrease in corrosion resistance of the alloy may be attributed to the complexation of degenerated HA molecular chains with chromium ions released from the metallic surface, which are necessary to build a protective oxide film. This finding has clinical implications, suggesting that HA accelerates corrosion of CoCrMo implants in the presence of strong inflammation.

Keywords

CoCrMo-alloy; corrosion; total joint replacement; hyaluronic acid; hydrogen peroxide

Corresponding author: Wimmer M. A., Tel. +1 312 942 2789, Fax +312 942 2040, < Markus_A_Wimmer@rush.edu >.

Disclosures

The authors have no conflicts of interest to declare.

1 Introduction

CoCrMo alloys, as defined by ISO 5832-12 (cast), ISO 5832-12 or ASTM F1537 (wrought), are used for components in hip and knee prostheses. CoCrMo alloys have outstanding mechanical and corrosion properties [1]. Their corrosion resistance (and thus biocompatibility) in body fluids relies on the presence of a protective surface oxide film [2]. Still, the use of CoCrMo as implant alloy is associated with the release of wear and corrosion debris that have been related to clinical problems, such as metal hypersensitivity [3], adverse local tissue reactions and finally implant failure [4, 5]. The mechanisms responsible for the body reactions to generated CoCrMo-debris need to be investigated using conditions, which approach the *in vivo* situation.

Hyaluronic acid (HA) is present in synovial joints, where it contributes to the lubrication of the opposing joint surfaces due to its high viscosity [6]. As an important component of synovial fluid, HA has been added to model lubricants in tribological and corrosion studies with articulating materials used in joint replacement [7–10]. From the clinical perspective, HA solutions have been injected into patients' knee joints in order to enhance lubrication and thus mitigate osteoarthritis [11, 12]. HA is a long, unbranched polysaccharide composed of alternating units of N-acetylglucosamine and glucuronic acid. Both moieties can give up anions, which could be used to reduce reactive oxygen species (ROS).

Hydrogen peroxide (H_2O_2) is one of the ROS species present *in vivo*. It has been used to simulate inflammatory conditions in tribological and tribocorrosion experiments for materials used in joint replacement [13–16]. During the inflammatory response, activated phagocytic leukocytes produce H_2O_2 and superoxide, which subsequently interact, forming hydroxyl radicals, singlet oxygen, and additional H_2O_2 [16]. While the exact levels of these chemistries *in vivo* are unknown, literature suggests that a concentration range of 0.1 mM to (locally) 30 mM is possible [13].

Besides the degradation of HA by excessive Reactive Oxygen Species (ROS) generated in pathologic joint synovial fluids [17], HA and synovial fluid were shown to exert antioxidant activities by scavenging ROS (H_2O_2, O^-_2, OH• and chemiluminescence) in a dose-dependent manner [18]. In particular, it has been shown that it is the D-glucuronic acid of the HA molecule that reacts with H_2O_2.

The importance of using more complex and thus more realistic solutions, as well as considering longer time periods when testing metals for orthopedic implants, has been recently highlighted in recent works about the synergistic effects of albumin and H_2O_2 on the corrosion resistance Ti6Al4V alloys [19, 20], and about a clinically relevant HA containing lubricant for wear testing of materials for total knee arthroplasty implants (UHMWPE/CoCr) [21]. In the same context, the effect of HA on the electrochemical and chemical changes promoted under sliding and its relation with the formation of in vitro tribochemical layers has been investigated for a CoCr/CoCr pin-on-disc system in phosphate buffer solution (PBS) [22].

To our knowledge, the combined effect of dissolved HA and H_2O_2 in a serum solution on the corrosion response of CoCrMo alloys has not yet been investigated. In this study, two

different concentrations of H_2O_2 (3 and 30 mM) were added to a physiological saline solution with 50% fetal bovine serum in the presence or absence of HA (3 g/L). Non-destructive, electrochemical methods were used to investigate the effect of these solutions on the corrosion behavior of a CoCrMo implant alloy used in total hip and knee replacement. Relatively long measurements (10 + 1 h) were carried out in order to test and compare the open circuit potential (OCP) evolution and stability. The rationale for long (10 h) OCP measurements was given by previous electrochemical experiments run in our lab and by other studies [7, 23], which report stabilization times up to 24 h for HA containing electrolytes. In addition, the protocol for the mixing of the HA powder (magnetically stirred in a cold room for 24 h) was chosen in order to assure complete HA dissolution and to promote the reproducibility of the measurements.

We hypothesized that, at an HA concentration value of 3 g/L, the oxidative effect of H_2O_2 up to equivalent molar concentrations (i.e., 7.5 mM) will be mitigated due to the redox capability of the HA molecule.

2 Materials and Methods

2.1. Metallic samples

Three discs made of low carbon (LC) CoCrMo (ASTM F1537), 12 mm in diameter and 7 mm in height, were embedded in acrylic resin forms (25 mm in diameter and 15 mm in height). A hole was drilled in the back of each acrylic form up to the metallic disc in order to establish electric contact in the three-electrode configuration. The specimens were polished with silicon carbide sand-paper up to 800/P1500 and cleaned in an ultrasonic bath (5 min in Tergazyme® detergent solution followed by 10 min in bidistilled water). Since each specimen was re-used five times, the polishing and cleaning was repeated before each test.

2.2. Electrolytes

The base solution used for all tests was composed of 51.6 vol% of saline sterile solution (0.9% sodium chloride, USP, Baxter Healthcare Corporation) and 48.4 vol% of newborn calf serum (Fischer Scientific, lot number 1751586) for a total protein concentration of 30 g/L. The HA was added in the form of sodium hyaluronate powder (Bulk Supplements (25g package, lot number 20150518) for a total concentration of 3 g/L. According to the supplier, the purity level of the HA powder was at least 96%. Additional analyses performed in our lab revealed a purity level of 97.1% and contamination values of 0.18% for proteins, 1.78% for lipids, 0.001% for DNA, and 2.69 EU/ml for endotoxins. This level of impurities was deemed acceptable for the purposes of this study. Hydrogen peroxide was added using a 35 wt% H_2O_2 ultrapure analytical reagent (Tamapure AA-10, metallic impurity level ≤ 10 ppt) for a final concentration of either 3 or 30 mM (0.29 or 2.9 g of reagent/L). The protein and HA concentrations used in this study are clinically relevant as they relate to the synovial fluid of patients after total hip replacement [6].

After preparation, the stock base solution was kept in the refrigerator at 5 °C for a maximum of 2 weeks and used to prepare six electrolytes for this study: To the base solutions containing no H_2O_2, 3 mM H_2O_2, and 30 mM H_2O_2 were added with or without HA (see

Table 1). All tests without HA were done first. For the HA containing electrolytes, HA powder was added to the remaining stock base solution and gently stirred for 24 h in a cold room (4 °C) for complete dissolution. For the H_2O_2 containing electrolytes, volumes of 2.58 and 25.8 μl (which respectively correspond to 3 mM H_2O_2 and 30 mM H_2O_2 considering the specific weight of the 35 wt% H_2O_2 reagent) were added to 10 ml of base solution, with or without HA, and stirred for 1 h at room temperature before the test. In all cases, the volume needed for each test (10 ml) was pipetted out from the stock solution and allowed to come to reach room temperature 1 h before the test was conducted. Three tests were performed for each electrolyte. The tests were performed at room temperature (21 ± 1 °C). No additives for pH control were used. The pH was measured before and after each test using an AB15 pH Meter (accumet® Basic, Fisher Scientific).

2.3. Electrochemical measurements

A three-electrode electrochemical configuration connected to a potentiostat (Interface 1000E, Gamry Instruments) was used to conduct the tests. The working electrode was the metal sample inside the acrylic specimen, exposing its surface to the electrolyte at the bottom of the chamber; the counter electrode was a platinum wire coiled above the working electrode; the reference electrode was a standard calomel electrode (0.241 V *vs.* SHE) placed through the coiled Pt wire. The chamber was sealed on the bottom with an O-ring and was covered on the top with a lid containing openings for the reference and counter electrode. This set-up avoided evaporation issues.

The test protocol consisted of the following sequence: (1) Open circuit potential (OCP) measurement (10 min); (2) Cathodic cleaning (−0.9 V *vs.* $E_{\mathbf{REF}}$, 10 min); 3) OCP measurement (60 min); (4) Linear Polarization Resistance (LPR) (200 s); (5) Electrochemical Impedance Spectroscopy (EIS). A loop of 10 cycles was set for steps 3 and 4, so that the OCP was measured for 10 h with an LPR measurement at the end of each hour. This means that the EIS measurement at the end of the sequence followed 10 h of OCP stabilization time. For the LPR measurements, the potential was scanned from −10 to +10 mV *vs.* E_{OC} at a rate of 0.1 mV/s. For the EIS measurements, the amplitude of the sinusoidal voltage perturbation was ±10 mV (rms) *vs.* E_{OC}, and the frequency ranged from 50 kHz to 0.05 Hz. The choice of the EIS parameters was based on published studies on similar systems [14, 24–26]. The Kramers-Kronig fit was applied to all EIS spectra for validation of the measurements. An equivalent circuit analysis was carried out using the Gamry Echem Analyst software (Version 6.33, Gamry Instruments).

In addition to the main protocol described above, a Tafel measurement, from −25 to +25 mV *vs.* E_{OC} and at a rate of 0.5 mV/s, was carried out after the first test of each electrolyte group. The Tafel measurements allowed for a quantitative estimation of the Tafel anodic and cathodic parameters (β_A and β_C) for each electrolyte group. These parameters were integrated into the LPR analysis for a quantitative estimation of corrosion rate values using the Gamry Echem Analyst software.

3 Results

The available pH values among all electrolytes (Table 2) remained in the range 7.5-8.3. A pH increase with time was observed along the duration of each test (ΔpH = 0.2-0.6).

The open circuit potential curves were obtained by stitching together the 10 × 1h measurements from 3 independent specimens for each electrolyte (Fig. 1). As can be observed from the curves, the initial behavior of OCP after cathodic polarization was not influenced by the presence or absence of HA (left column: no HA; right column: HA); however, it was influenced by the presence and concentration of H_2O_2 (top row: no H_2O_2; middle row: H_2O_2 [3 mM]; bottom row: H_2O_2 [30 mM]). The time necessary to reach the stationary open circuit potential decreased with increasing H_2O_2, which is seen by the increased slope of the potential evolution on the onset of the OCP measurement following the cathodic cleaning. According to [27], this time is an important characteristic of a passivating process and is associated with the electrochemical reactivity of the tested material in the test electrolyte. This is as expected from the catalyzing effect of H_2O_2. In the case of HA + 30 mM H_2O_2, the OCP showed an initial peak. The OCP values reached stable values at the end of the 10 h for all electrolytes. The difference between maximal and minimal potential values during the last (10^{th}) hour ranged from 4 to 12 mV/h. The presence of H_2O_2 tended to accelerate the OCP stabilization (accelerated passive film formation). The OCP curves from the tests in the electrolytes with 30 mM H_2O_2 only showed a noise-like behavior, which did not occur in the presence of HA. Base OCP values (without HA) are consistent with previously reported values of CoCrMo in serum of −0.2 V vs. SCE [25]. The increasing OCP values in the presence of H_2O_2 but without HA are also consistent with previously reported behavior for CoCrMo exposed to different concentrations (from 0.1 to 30 mM) of H_2O_2 in PBS [14]. T-Tests (Two-Sample Assuming Unequal Variances) on the final OCP values showed statistical difference ($p < 0.05$) between the groups Base *vs.* Base +3mM H_2O_2 ($p = 0.0128$), Base *vs.* Base+30mM H_2O_2 ($p = 0.0081$) and Base+3mM H_2O_2 *vs.* Base+30mM H_2O_2 (0.0499). On the other hand, there was no statistical difference among the groups with HA (p = 0.3699, p = 0.1023, and p= 0.3178 respectively).

Polarization resistance (R_p) values were calculated from the LPR measurements that were performed every hour for 10 h. For this calculation, a linear fit with correlation coefficient $R \geq 0.9$ was applied to the measured current in a window of ±2mV potential around the OCP, and the slope of this linear fit was converted into the units of measurement for specific R_p, kΩ cm^2 (Fig. 2). Note that the different OCP values for each electrolyte are in line with the average values reported in Table 3. No clear trend of either increase or decrease of R_p with time was observed. For this reason, the final R_p value (after 10 h) was considered for a comparative analysis among the groups. The polarization resistance decreased with increasing H_2O_2 concentration for both electrolyte groups with or without HA. The electrolyte with HA and 30 mM H_2O_2 showed a significantly lower polarization resistance compared to all others. Average and standard deviation values of R_p after 10 h are given in Table 3. T-Tests (Two-Sample Assuming Unequal Variances) on the final R_p values showed statistical difference ($p < 0.05$) only between the group Base+HA+3mM H_2O_2 *vs.* Base+HA +30 mM H_2O_2 ($p = 0.0337$), and the difference between Base+HA *vs.* Base+HA+30 mM H_2O_2 was nearly statistically significant ($p = 0.0691$). The critical behavior of this

electrolyte in terms of corrosion resistance is also reflected in the calculated corrosion rate values (Table 3). The corrosion rate increased with increasing H_2O_2 concentration as expected [14]. Unexpectedly, the presence of HA in 30 mM H_2O_2 electrolytes caused a 2-3 times increase of the corrosion rate.

The trend of decreased corrosion resistance with increasing H_2O_2 concentration seen in the OCP and LPR results was confirmed by the EIS measurements performed at the end of the test protocol (Fig. 3); this is clear by the decreased diameter of the semi-circle arcs in the Nyquist plots. The plots from the tests with HA and 30 mM H_2O_2 showed consistently a different behavior in the lower half of the frequency range. In order to investigate this, an equivalent circuit model analysis was carried out (parameters in Table 4, equivalent circuit in Fig. 4). This five-component model, which has been used by other authors with a similar system [25, 28], allowed the fitting of 17 of the 18 EIS measurements. The Chi-squared values (the squared sum of weighted residuals, also called Goodness of Fit) reported in the last column of Table 4 are in the order of magnitude of 1E-04 and 1E-05, documenting a very good fit of the model circuit; in fact, published works in the field report Chi-squared values in the order of magnitude of 1E-03 [29] and 1E-0.2 [28] (the lower the Chi-squared value, the better the fit). The model was able to calculate the values for the resistance elements at the lowest frequencies, despite most of the measurements did not reach a steady state resistance (impedance given only by the real part). This behavior has been observed by other authors with similar systems [14, 24–26]; in particular, the extrapolation of the resistive element at lower frequencies can be clearly seen in [24]. The solution resistance was in the range (53 ± 5) Ω cm^2 for all electrolytes. The CPE of the adsorbed layer was characterized by alpha values equal to 0.9 for all electrolytes, meaning that the adsorbed layer can be associated with a capacitor. As can be seen by comparing the values of CPE coefficient of the adsorbed layer (Q_{al}) in Table 4, Q_{al} was not influenced by the presence of HA and tended to slightly decrease with increasing H_2O_2 concentration. The resistance of the adsorbed layer did not show a clear trend and was in the range of 4 −7 kΩ cm^2 for all electrolytes, with the exception of the second simulation for the electrolyte “Base + HA + 30 mM H_2O_2”. Nevertheless, this simulation showed a relatively high value of the Chi Squared, which means that this fit was relatively poor. At the electrode-electrolyte interface, the CPE coefficient of the double layer (Q_{dl}) and the charge transfer resistance (R_{ct}) were simulated. However, the CPE of the double layer was characterized by alpha values equal to 0.5 ± 0.1 for all electrolytes. The alpha value can be associated with a distribution of time constants along the surface, meaning non-uniform current and potential distributions. In this model, a non-uniform adsorption of proteins could be reflected in the capacitance behavior of the surface double layer with low alpha values.

This interpretation is supported by the fact that the protein concentration was the same for all electrolytes and the values of Q_{dl} did not show a clear trend among all electrolytes. The simulated charge transfer resistance was in the range of 110 – 589 kΩ·cm^2 for the first five groups, excluding the value above 3000 kΩ·cm^2 from the first simulation in the group “Base + HA” with relatively high Chi Squared. For “Base + HA + 30 mM H_2O_2”, R_{ct} values were up to one order of magnitude smaller (29 – 55 kΩ·cm^2).

4 Discussion

This study investigated whether the redox capability of HA, a main component in synovial fluid, could mitigate corrosion of CoCrMo implant alloy under inflammatory conditions. Inflammation was modelled in this study by the addition of 3 mM or 30 mM H_2O_2 to a proteinaceous testing fluid. Using EIS and LPR measurements, calculating the polarization resistance and corrosion rate after 10 h of OCP stabilization, we did not find evidence for the hypothesized scavenging of H_2O_2 by an antioxidant action of HA for the 3 mM H_2O_2 condition. While statistical differences of stable OCP values were found among the groups with different molarities of H_2O_2 in the absence of HA, no statistical differences with different molarities of H_2O_2 were found when HA was present; on the contrary, statistical significant differences were found in the polarization resistance values, showing the influence of H_2O_2 also in the presence HA. According to pH measurements, the electrolytes used in this study tended to turn basic with time, with no clear influence of H_2O_2 and HA. We conclude, that the behavior of the system is a matter of the considered size scale: the pH values reflect the properties of the bulk solution; the stable OCP values reflect an unchallenged state of the CoCrMo surface, that is, a surface with relatively stable double-layer; the LPR and EIS values reflect the electrochemical response of the surface even to small (± 10 mV) amplitude voltage signals, therefore including possible interactions among HA and H_2O_2 molecules at the CoCrMo surface, within the double-layer.

The surface of the CoCrMo alloy is protected by a natural, uniform oxide film, which is composed mainly of Cr_2O_3 [2]. The isoelectric point of Cr_2O_3 is in the range of 6.2-8.1 [30]. The isoelectric point of HA is 2.5 [31]. The measured pH of the electrolytes was 7.5-8.2. Based on these values, it can be assumed that no electrostatic attraction of the HA molecules towards the metallic surface occurred during our experiments. In fact, the metallic surface had a neutral charge, while the HA molecules were negatively charged. On the other hand, the metallic surface was certainly covered by proteins, because proteins from biological fluids are known to adsorb onto biomaterial surfaces almost instantaneously [26, 32, 33]. The additional presence of H_2O_2 likely caused an oxidation of the metal surface through the adsorbed protein layer with growth of an unstable (porous) oxide film. This assumption is supported by our results as the OCP increases and the corrosion resistance decreases, as well as by other studies in literature [13]. In this context, the physiological concentration of 3 g/l HA showed no antioxidant effect on the corrosion behavior of the CoCrMo implant alloy at 3 mM H_2O_2.

The adsorbed layer of proteins and/or a porosity in the protective oxide film caused by H_2O_2 is reflected by the second time constant in the phase diagram of the Bode plots. The second time constant was observed for all electrolyte groups except for “Base + HA + 30 mM H_2O_2”, suggesting that the kinetics of the electrochemical reactions occurring at the metallic surface in this electrolyte were not disturbed by adsorbed layers or by a porous protective film. In fact, all electrochemical methods and calculations presented here indicated a significantly reduced corrosion resistance with the group “Base + HA + 30 mM H_2O_2”, as compared to the other groups, including the group “Base + 30 mM H_2O_2”. According to the EIS equivalent circuit simulation, this drastic decrease in corrosion resistance was due to a decrease in charge transfer resistance at the CoCrMo surface. The charge transfer resistance

values of the EIS simulation were reflected in the polarization resistance values calculated from the LPR measurements. Despite the different electrochemical derivation of these two parameters, the resistance to charge transfer may be seen as a contribution to the polarization resistance (the polarization resistance is measured over a larger voltage range and may also include the diffusion resistance of the reactants). Additional measurements in 0.9% NaCl solutions with HA and 30 mM H_2O_2, using the same protocol as for all the other tests, yielded EIS Bode plots indicating that the absence of proteins generated a behavior of pure diffusion at the CoCrMo surface, with no resistance elements (Fig. 5). This confirmed that HA in combination with H_2O_2 [30 mM] has the effect of accelerating the electrochemical reactions at the CoCrMo surface.

A possible explanation for this finding is the following: the high concentration of H_2O_2 and the contact to the metallic surface promote the rupture of the HA chains by the action of hydroxyl radicals through Fenton-like reaction [34, 35]. At the same time, H_2O_2 oxidizes the CoCrMo surface with production of Co^{2+}/Cr^{3+} ions and hydroxyl radicals. It is possible, in this condition, that the protein layer is partially removed from the surface and that HA molecules present in a volume close enough to the surface complex with released Co^{2+}/Cr^{3+} ions, transporting them away from the surface. The resulting oxide film is thus depleted of CoO/Cr_2O_3 and, consequently, it becomes less protective in the presence of HA than in the absence of it. This difference in the quality of the protective film was also reflected in the OCP measurements: the OCP reached higher values in 30 mM H_2O_2 without HA, indicating a higher rate of oxide film growth, as compared to the 30 mM H_2O_2 electrolyte with HA.

Although we found no reports detailing complex formation of hyaluronate with Cr^{3+} or Co^{2+}, it has been shown that ferric ion, another 3d transition metal ion, reacts with hyaluronate ion in aqueous solution to from $Fe3^{+}$-hyaluronate complexes through both the N-glucosamine and D-glucoronic acid moieties [36]. Furthermore, the above described hypothesis is supported by literature about the effect of different metal ions on the oxidative damage and antioxidant capacity of hyaluronic acid [35]. In this study, bivalent metallic ions were shown to preferentially associate to HA, forming structure-stabilizing complexes and preventing their ROS-induced degradation. Interestingly, the recruitment of the Cr^{3+} ions by the HA forming Metal-HA complexes has also been speculated to be the explanation for higher wear rates observed with CoCr/UHMWPE in a knee simulator in HA containing bovine serum lubricants, as compared to bovine serum lubricants only [21]. Finally, according to the results from a very recent study [22], the fraction of chromium oxide $Cr(OH)_3$ in the passive film of a CoCr alloy exposed to PBS with 0.3% HA decreased under the tested wear conditions, suggesting that HA preferentially interacts with chromium with a consequent net loss in available chromium within the passivating layer. We therefore speculate, that the decrease in corrosion resistance in the presence of HA and 30 mM H_2O_2 observed in the present study may be caused by a similar degeneration process of the protective passive layer of the CoCrMo alloy already observed under wear conditions in the presence of HA [21, 22]. Further investigation is warranted as this finding may have a critical, clinical implication suggesting that, in cases of extreme inflammation, HA may accelerate *in vivo* corrosion of CoCrMo implants.

This study documents the initial investigations performed in our laboratory about interactions between HA as a main synovial fluid component and H_2O_2 as an inflammatory simulating species in an orthopedic, tribocorrosion system with CoCrMo alloy. The study is not without limitations: (1) the number of H_2O_2 concentration values tested is insufficient to give information about the threshold value where the change in corrosion behavior occurs; (2) the clinical relevance of the highest value tested (30 mM H_2O_2) has no *in vivo* proof; (3) it was not possible to distinguish differences between diffusion effects given by proteins adsorbed on the CoCrMo surface from those given by porosity in the protective oxide film generated by H_2O_2 oxidation; (4) the electrochemical measurements used in this study are non-destructive: the corrosion resistance of the surface in the different media was evaluated indirectly, without accelerating corrosion of the surface through anodization, tribocorrosion or longer (over several days) immersion tests. In this context, it was possible to re-use a limited amount of the samples, which were available for the study. To ensure the same initial surface conditions for each test, samples were re-polished, and cleaned both in ultrasonic bath and electrochemically (cathodic cleaning). Nevertheless, the methodology chosen did not allow for direct analysis of corrosion-rate and -mechanism, including changes in the samples' weight, in surface morphology, surface roughness or surface composition. Therefore, despite the clinically relevant concentration of HA and proteins and the use of a medical alloy, this study claims no clinically relevant statements. Possible mechanisms involved in the influence of HA and H_2O_2 in the corrosion behavior of CoCrMo require further investigation. The use of destructive electrochemical methods and/or microelectrodes in future experiments might be promising in this context. As next step, we will perform fretting corrosion tests using the same lubricants and we will include a more accurate the analysis of the different media tested, assessing degradation rates of the HA and H_2O_2 molecules.

5 Conclusions

- The various electrochemical techniques employed (OCP, LPR, EIS) delivered consistent results.
- The addition of HA to a serum saline solution in concentrations representative of synovial fluid showed a minor influence on the corrosion behavior of the CoCrMo alloy (slightly decreasing corrosion resistance).
- The addition of 3 mM H_2O_2 representing moderate inflammation conditions caused a further moderate decrease in corrosion resistance, independently of the presence of HA.
- In contrast, 30 mM H_2O_2 and the presence of HA caused a major decrease in corrosion resistance of the CoCrMo alloy. This finding can be explained by a decrease in the protective quality of the passive film, due to the degradation of the HA molecules caused by H_2O_2, combined with complexation of HA chains with metal ions released from the CoCrMo surface, thus potentially causing chromium depletion in the oxide film.

Acknowledgements

The authors would like to thank the following Rush colleagues for their very helpful collaboration: Drs. Nadim J. Hallab, Tom Schmid, Deborah J. Hall, and Anastasia K. Skipor. Finally, thanks to Dr. M. T. Mathew and The Blazer Foundation for the use of the Interface 1000E potentiostat.

Funding

This work was partially supported by the National Institutes of Health [NIH/NIBIB R21 EB024039].

REFERENCES

[1]. Aherwar A, Singh A, Patnaik A, Cobalt Based Alloy: A Better Choice Biomaterial for Hip Implants, Trends Biomater. Artif. Organs 30(1) (2016) 50–55.

[2]. Valero-Vidal C, Igual Muñoz A, Olsson C-OA, Mischler S, Passivation of a CoCrMo PVD Alloy with Biomedical Composition under Simulated Physiological Conditions Studied by EQCM and XPS, Journal of The Electrochemical Society 159(5) (2012) C233–C243.

[3]. Hallab N, Merritt K, Jacobs JJ, Metal sensitivity in patients with orthopaedic implants, J Bone Joint Surg Am 83-A(3) (2001) 428–36.

[4]. Hart AJ, Quinn PD, Lali F, Sampson B, Skinner JA, Powell JJ, Nolan J, Tucker K, Donell S, Flanagan A, Mosselmans JFW, Cobalt from metal-on-metal hip replacements may be the clinically relevant active agent responsible for periprosthetic tissue reactions, Acta Biomaterialia 8(10) (2012) 3865–3873. [PubMed: 22688088]

[5]. Hart AJ, Quinn PD, Sampson B, Sandison A, Atkinson KD, Skinner JA, Powell JJ, Mosselmans JFW, The chemical form of metallic debris in tissues surrounding metal-on-metal hips with unexplained failure, Acta Biomaterialia 6(11) (2010) 4439–4446. [PubMed: 20541630]

[6]. Bortel E, Charbonnier B, Heuberger R, Development of a Synthetic Synovial Fluid for Tribological Testing, Lubricants 3(4) (2015) 664.

[7]. Hirzallah RRW, Corrosion Behavior of Co28Cr6Mo Implant in the Presence of Bovine Serum Albumin and Hyaluronic Acid, Materials Engineering, Master Thesis at The University of British Columbia, Vancouver, 2014.

[8]. Diomidis N, Mischler S, More NS, Roy M, Paul SN, Fretting-corrosion behavior of β titanium alloys in simulated synovial fluid, Wear 271(7-8) (2011) 1093–1102.

[9]. Gispert M, Serro A, Colaco R, Saramago B, Friction and wear mechanisms in hip prosthesis: Comparison of joint materials behaviour in several lubricants, Wear 260(1) (2006) 149–158.

[10]. More NS, Diomidis N, Paul SN, Roy M, Mischler S, Tribocorrosion behavior of β titanium alloys in physiological solutions containing synovial components, Materials Science and Engineering: C 31(2) (2011) 400–408.

[11]. Weick JW, Bawa HS, Dirschl DR, Hyaluronic Acid Injections for Treatment of Advanced Osteoarthritis of the Knee: Utilization and Cost in a National Population Sample, J Bone Joint Surg Am. 98(17) (2016) 1429–35. [PubMed: 27605686]

[12]. Maheu E, Bannuru RR, Herrero-Beaumont G, Allali F, Bard H, Migliore A, Why we should definitely include intra-articular hyaluronic acid as a therapeutic option in the management of knee osteoarthritis: Results of an extensive critical literature review, Semin Arthritis Rheum 48(4) (2019) 563–572. [PubMed: 30072113]

[13]. Liu Y, The effects of simulated inflammatory conditions on the corrosion and fretting corrosion of CoCrMo alloy, Biomedical and Chemical Engineering, PhD thesis at the Syracuse University, 2017.

[14]. Gilbert JL, Sivan S, Liu Y, Kocagoz SB, Arnholt CM, Kurtz SM, Direct in vivo inflammatory cell-induced corrosion of CoCrMo alloy orthopedic implant surfaces, J Biomed Mater Res A 103(1) (2015) 211–23. [PubMed: 24619511]

[15]. Pan J, Thierry D, Leygraf C, Hydrogen peroxide toward enhanced oxide growth on titanium in PBS solution: blue coloration and clinical relevance, J Biomed Mater Res 30(3) (1996) 393–402. [PubMed: 8698703]

[16]. Montague A, Merritt K, Brown S, Payer J, Effects of Ca and H2O2 added to RPMI on the fretting corrosion of Ti6Al4V, J Biomed Mater Res 32(4) (1996) 519–26. [PubMed: 8953141]

[17]. Jahn M, Baynes JW, Spiteller G, The reaction of hyaluronic acid and its monomers, glucuronic acid and N-acetylglucosamine, with reactive oxygen species, Carbohydr Res 321(3-4) (1999) 228–34. [PubMed: 10614067]

[18]. Sato H, Takahashi T, Ide H, Fukushima T, Tabata M, Sekine F, Kobayashi K, Negishi M, Niwa Y, Antioxidant activity of synovial fluid, hyaluronic acid, and two subcomponents of hyaluronic acid. Synovial fluid scavenging effect is enhanced in rheumatoid arthritis patients, Arthritis Rheum 31(1) (1988) 63–71. [PubMed: 3345232]

[19]. Yu F, Addison O, Davenport AJ, A synergistic effect of albumin and H2O2 accelerates corrosion of Ti6Al4V, Acta Biomaterialia 26 (2015) 355–365. [PubMed: 26238758]

[20]. Zhang Y, Addison O, Yu F, Rincon Troconis B, Scully JR, Davenport A, Time-dependent Enhanced Corrosion of Ti6Al4V in the Presence of H2O2 and Albumin, Scientific Reports 8(1) (2018) 3185. [PubMed: 29453366]

[21]. DesJardins J, Aurora A, Tanner SL, Pace TB, Acampora KB, Laberge M, Increased total knee arthroplasty ultra-high molecular weight polyethylene wear using a clinically relevant hyaluronic acid simulator lubricant, Proc Inst Mech Eng H. 220(5) (2006) 609–23. [PubMed: 16898218]

[22]. Garcia-Alonso MC, Llorente I, Diaz I, Escudero ML, Interaction of Hyaluronic Acid with CoCr Alloy Under Immersion and Wear - Corrosion Processes, Tribology Letters 66(4) (2018) 122.

[23]. Milošev I, Hmeljak J, Cör A, Hyaluronic acid stimulates the formation of calcium phosphate on CoCrMo alloy in simulated physiological solution, Journal of Materials Science: Materials in Medicine 24(3) (2013) 555–571. [PubMed: 23250579]

[24]. Muñoz AI, Mischler S, Interactive Effects of Albumin and Phosphate Ions on the Corrosion of CoCrMo Implant Alloy, Journal Of The Electrochemical Society 154(10) (2007) C562–C570.

[25]. Ouerd A, Alemany-Dumont C, Normand B, Szunerits S, Reactivity of CoCrMo alloy in physiological medium: Electrochemical characterization of the metal/protein interface, Electrochimica Acta 53(13) (2008) 4461–4469.

[26]. Valero Vidal C, Olmo Juan A, Igual Munoz A, Adsorption of bovine serum albumin on CoCrMo surface: effect of temperature and protein concentration, Colloids Surf B Biointerfaces 80(1) (2010) 1–11. [PubMed: 20554436]

[27]. Ponthiaux P, Wenger F, J-P C., Tribocorrosion: Material Behavior Under Combined Conditions of Corrosion and Mechanical Loading, in: Shih (Ed.), Corrosion Resistance2012.

[28]. Lavos-Valereto IC, Wolynec S, Ramires I, Guastaldi AC, Costa I, Electrochemical impedance spectroscopy characterization of passive film formed on implant Ti–6Al–7Nb alloy in Hank's solution, Journal of Materials Science: Materials in Medicine 15(1) (2004) 55–59. [PubMed: 15338591]

[29]. Barao VA, Mathew MT, Assuncao WG, Yuan JC, Wimmer MA, Sukotjo C, Stability of cp-Ti and Ti-6Al-4V alloy for dental implants as a function of saliva pH - an electrochemical study, Clin Oral Implants Res 23(9) (2012) 1055–62. [PubMed: 22092540]

[30]. Scientific H, Determination of the Isoelectric Point Using Zeta Potential, Saved from URL: https://www.azom.com/article.aspx?ArticleID=5829 (2011).

[31]. Gatej I, Popa M, Rinaudo M, Role of the pH on Hyaluronan Behavior in Aqueous Solution, Biomacromolecules 6(1) (2005) 61–67. [PubMed: 15638505]

[32]. Silva-Bermudez P, Rodil S, An Overview on Protein Adsorption on Metal Oxide Coatings for Biomedical Implants, 2013.

[33]. Yan Y, Yang H, Su Y, Qiao L, Albumin adsorption on CoCrMo alloy surfaces, Scientific Reports 5 (2015) 18403. [PubMed: 26673525]

[34]. Miyazaki T, Yomota C, Okada S, Degradation of hyaluronic acid at the metal surface, Colloid & Polymer Science 276 (1998) 388–394.

[35]. Balogh GT, Illés J, Székely Z, Forrai E, Gere A, Effect of different metal ions on the oxidative damage and antioxidant capacity of hyaluronic acid, Archives of Biochemistry and Biophysics 410(1) (2003) 76–82. [PubMed: 12559978]

[36]. Merce AL, Marques Carrera LC, Santos Romanholi LK, Lobo Recio MA, Aqueous and solid complexes of iron(III) with hyaluronic acid. Potentiometric titrations and infrared spectroscopy studies, J Inorg Biochem 89(3-4) (2002) 212–8. [PubMed: 12062125]

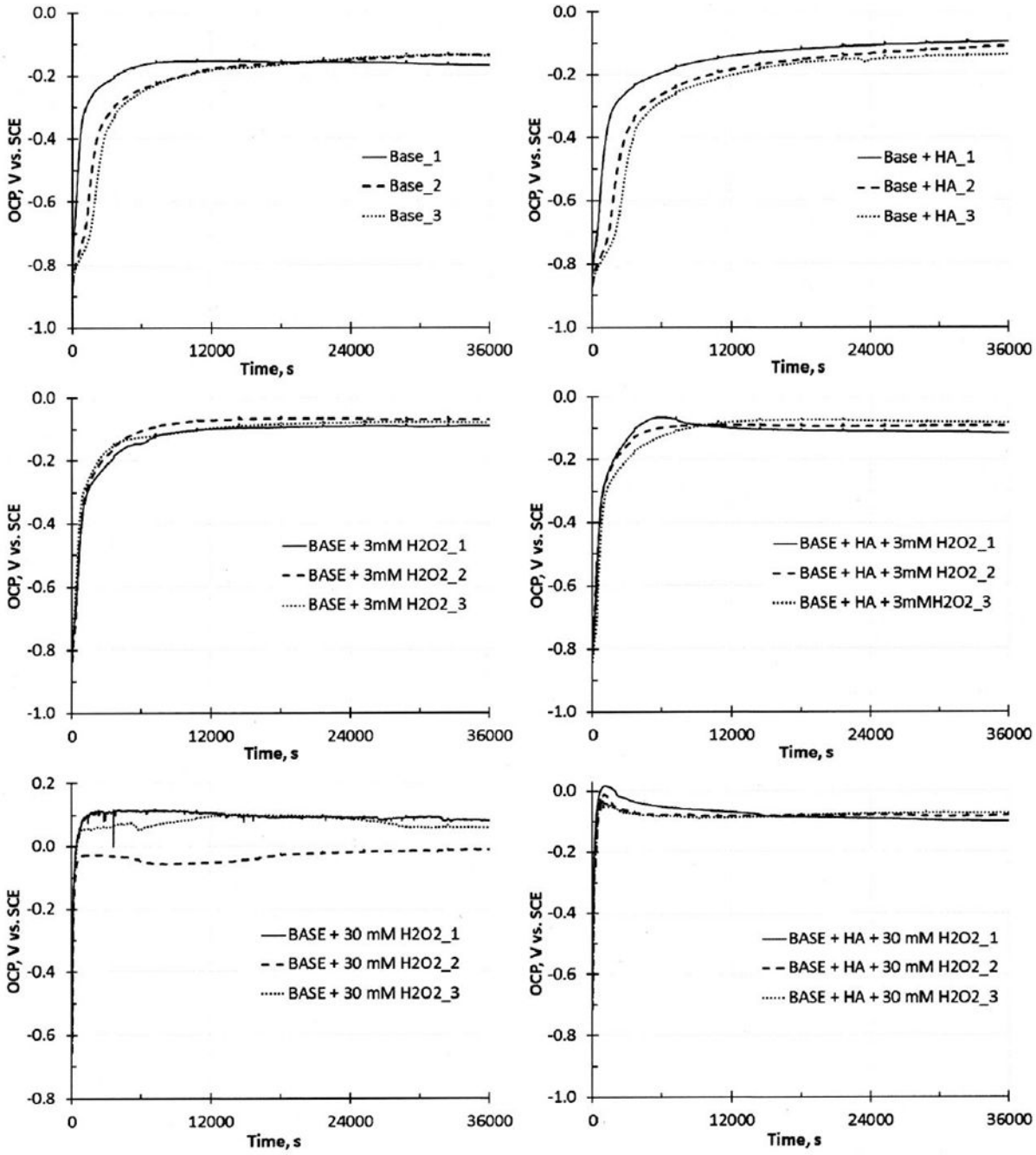

Fig. 1.

Open Circuit Potential curves, obtained by stitching together the 10×1h measurements on 3 independent specimens, with the electrolytes described in Table 1: without HA on the left; with HA on the right; without H_2O_2 on the top; with 3 mM H_2O_2 in the middle; with 30 mM H_2O_2 on the bottom.

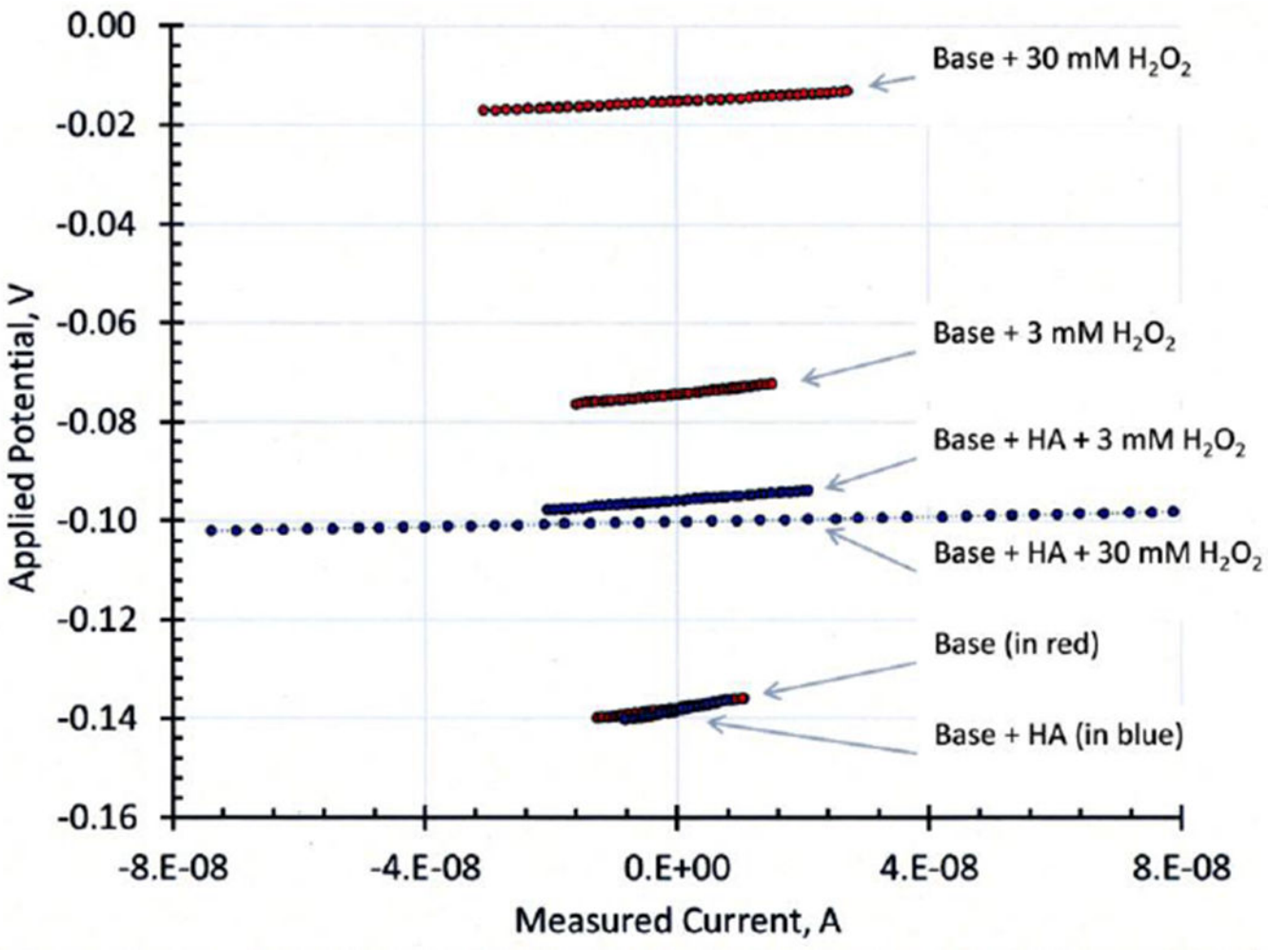

Fig. 2.

Current measurements during LPR in a window of ± 2mV around the OCP, used for the calculation of R_p: the slopes of linear fits with correlation coefficient ≥ 0.9 were converted into units of specific R_p (one test per group; in the online version, data in red correspond to electrolytes without HA and, in blue, to electrolytes with HA). The different OCP values for each electrolyte are in line with the average values reported in Table 3.

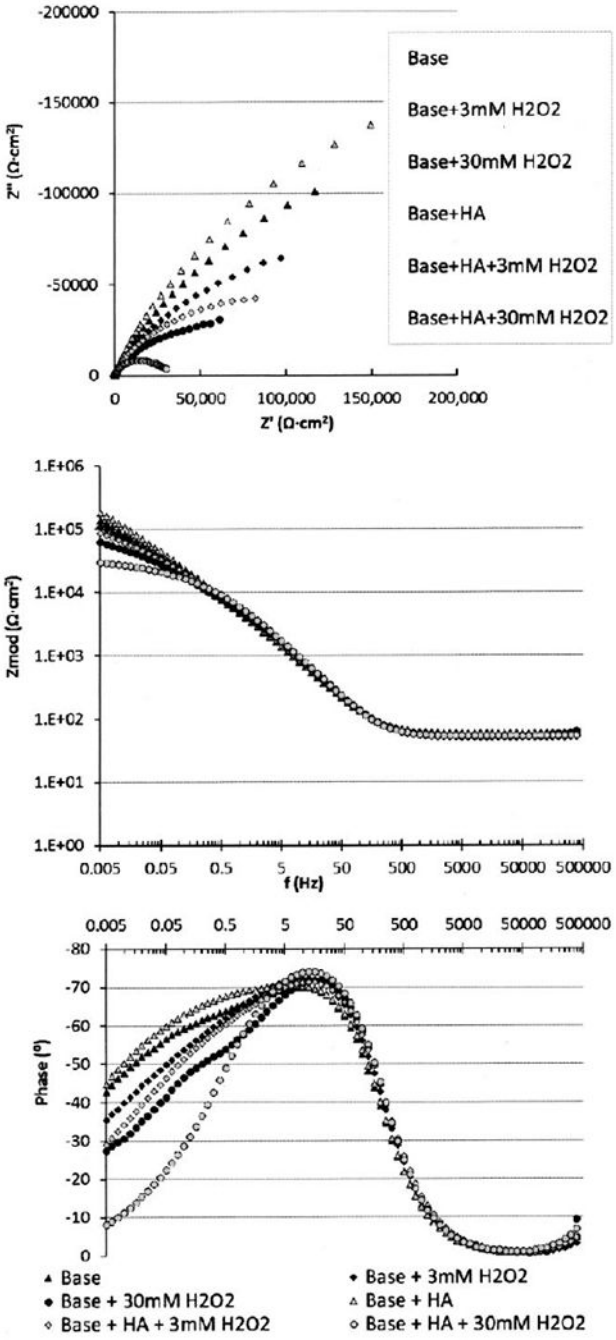

Fig. 3.

Representative Nyquist (top), Bode module (middle), and Bode phase (bottom) plots resulting from the Electrochemical Impedance Spectroscopy measurements for the electrolyte groups described in Table 1.

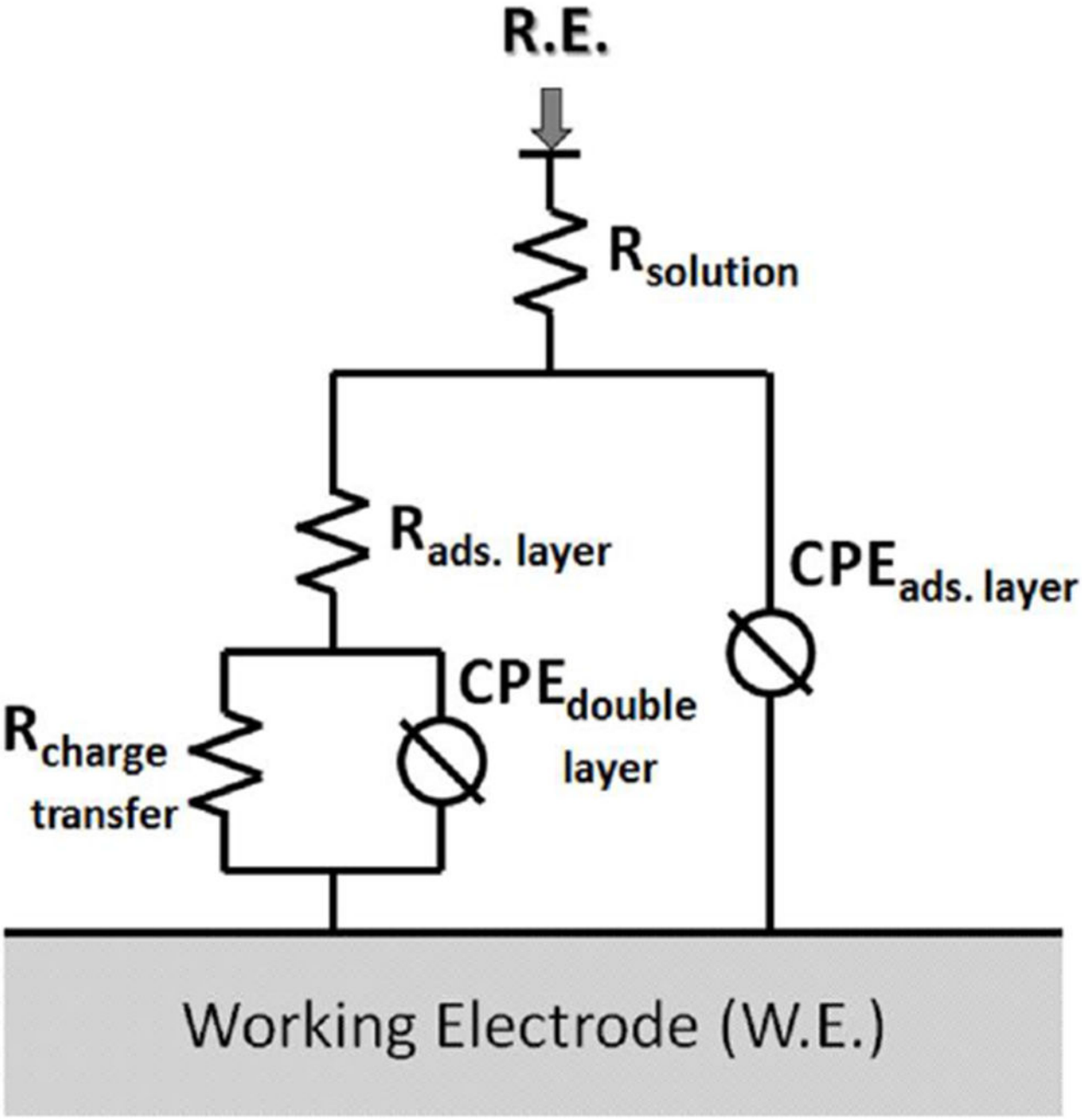

Fig. 4.
Equivalent electric circuit model used to fit the EIS plots presented in Fig. 3.

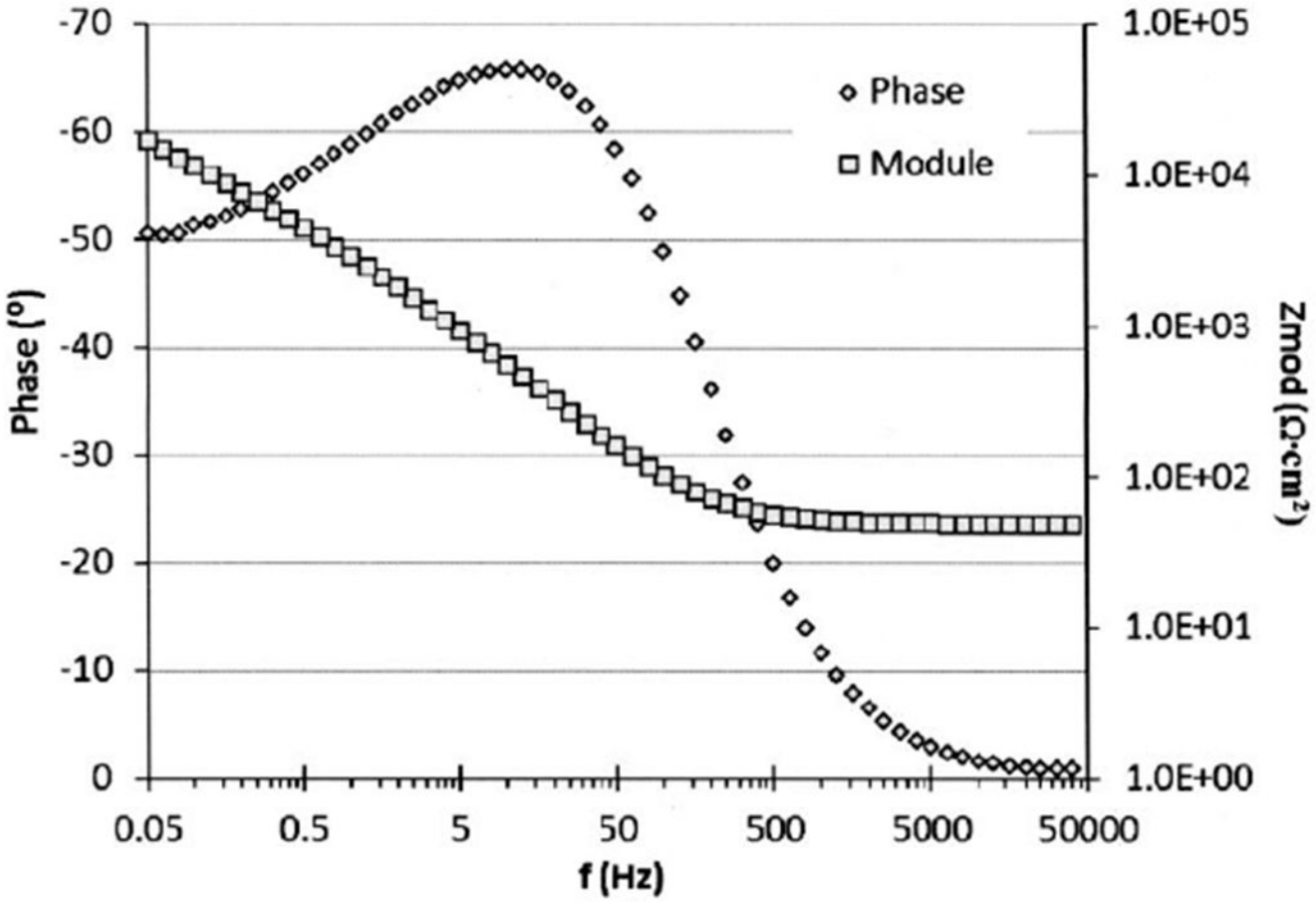

Fig. 5.

Bode plots from EIS measurements with 0.9% NaCl solution + HA [3g/l] + H2O2 [30 mM]. They are consistent with pure diffusion at the CoCrMo surface with no resistance elements.

Table 1.

The 6 different electrolytes tested in this study. The base solution was composed of 51.6 vol% of saline sterile solution and 48.4 vol% of newborn calf serum, for a total protein concentration of 30 g/L.

HA	H_2O_2		
	None	**3 mM**	**30 mM**
-	Base	Base + 3mM H_2O_2	Base + 30 mM H_2O_2
3 g/L	Base + HA	Base + HA + 3 mM H_2O_2	Base + HA + 30 mM H_2O_2

Table 2.

Measurements of pH before and after each test.

Electrolyte	Test #	pH before	pH after	ΔpH
Base	1	7.55	8.05	0.50
	2	7.47	8.05	0.58
	3	-	8.20	-
Base+ **HA**	1	-	8.32	-
	2	-	8.18	-
	3	-	8.10	-
Base+ 3mM H_2O_2	1	7.60	8.15	0.55
	2	7.86	8.15	0.29
	3	7.94	8.35	0.41
Base+ **HA**+ 3mM H_2O_2	1	7.48	8.01	0.53
	2	7.83	8.14	0.31
	3	7.97	8.29	0.32
Base+ 30mM H_2O_2	1	7.80	8.20	0.40
	2	7.80	8.26	0.46
	3	7.81	8.33	0.52
Base+ **HA**+ 30mM H_2O_2	1	8.03	8.28	0.25
	2	8.14	8.33	0.19
	3	8.23	8.42	0.19

Table 3.

Average and corresponding standard deviation of open circuit potential (OCP) values (V vs. SCE), polarization resistance (R_p) values ($k\Omega \cdot cm^2$), and corrosion rate (vcorr) values (microns per year) derived from OCP and LPR measurements, relative to the CoCrMo specimens after 10 hours (electrolytes described in Table 1). The Tafel parameters used for the calculation of the corrosion rate were extracted from separate Tafel measurements (not shown), performed at the end of the first test of each electrolyte group.

Electrolyte	**OCP ± st. dev., V *vs.* SCE**	**R_p ± st. dev., $k\Omega \cdot cm^2$**	**v_{corr} ± st. dev., $\mu m \cdot y^{-1}$**
Base	− 0.15 ± 0.019	182 ± 86	1.6 ± 0.9 (β_A, β_C = 0.10)
Base+ **HA**	− 0.11 ± 0.020	208 ± 76	1.3 ± 0.5 (β_A, β_C = 0.10)
Base+ 3mM H_2O_2	− 0.08 ± 0.010	137 ± 8	2.2 ± 0.2 (β_A, β_C = 0.12)
Base+ **HA**+ 3mM H_2O_2	− 0.10 ± 0.017	112 ± 26	2.3 ± 0.6 (β_A, β_C = 0.10)
Base+ 30mM H_2O_2	+ 0.04 ± 0.048	116 ± 34	2.8 ± 1.1 (β_A, β_C = 0.12)
Base+ **HA**+ 30mM H_2O_2	− 0.08 ± 0.014	46 ± 11	7.8 ± 3.0 (β_A, β_C = 0.13)

Table 4.

Parameters of the equivalent circuit given in Fig. 4 calculated by fitting the EIS plots of Fig. 3 (electrolytes described in Table 1).

Electrolyte	R_s, Ωcm^2	Q_{al}, μSs$^{\alpha}$/cm^2	α_{al}, -	R_{al}, kΩcm^2	Q_{dl}, μSs$^{\alpha}$/cm^2	α_{dl}, -	R_{ct}, kΩcm^2	Chi Squared, -
Base	55 58 58	44 33 27	0.9 0.9 0.9	5 5 3	87 32 28	0.6 0.6 0.6	143 466 553	1.60E-04 1.45E-05 9.13E-05
Base+ **HA**	51 - 58	35 - 28	0.9 - 0.9	4 - 2	55 - 26	0.5 - 0.6	3187 - 589	1.18E-04 no fit 1.92E-05
Base+ 3mM H_2O_2	53 52 51	29 30 29	0.9 0.9 0.9	2 6 2	22 35 26	0.5 0.5 0.5	174 337 171	1.86E-04 2.03E-05 1.16E-04
Base+ **HA**+ 3 mM H_2O_2	55 49 49	32 28 28	0.9 0.9 0.9	4 4 4	38 37 26	0.5 0.5 0.5	110 180 277	3.19E-05 2.29E-05 8.42E-05
Base+ 30mM H_2O_2	55 53 53	22 23 21	0.9 0.9 0.9	4 4 7	21 54 27	0.5 0.5 0.6	168 120 214	4.30E-04 1.57E-04 1.67E-04
Base+ **HA**+ 30 mM H_2O_2	52 55 50	23 20 20	0.9 0.9 0.9	7 35 6	52 73 28	0.6 0.6 0.4	29 39 55	3.39E-05 4.18E-04 1.41E-04